NANO LETTERS

2007
Vol. 7, No. 10
3219−3222

Localized Electron States near a Metal/Semiconductor Nanocontact

Denis O. Demchenko* and Lin-Wang Wang

Computational Research Division, Lawrence Berkeley National Laboratory, Berkeley, California 94720

Received August 13, 2007; Revised Manuscript Received September 6, 2007

ABSTRACT

The electronic structure of nanowires in contact with metallic electrodes of experimentally relevant sizes is calculated by incorporating the electrostatic image potential into the atomistic single particle Schrödinger equation. We show that the presence of an electrode produces localized electron/hole states near the electrode. We found a strong nanowire size dependence of this localization effect. We calculate several electrode/nanowire geometries, with varying contact depths and nanowire radii. We demonstrate the change in the band gap of up to 0.5 eV in 3 nm diameter CdSe nanowires and calculate the magnitude of the applied electric field necessary to overcome the localization.

The properties of metal/nanostructure contacts, especially the new phenomena unique to the nanostructures, are of great importance to the future of nanoelectronics and are currently intensively studied. A variety of nanostructures is being fabricated, ranging from quantum dots to sophisticated structures such as tetrapods, nanoribbons, etc.[1−3] Transport measurements in these nanostructures are often conducted by contacting a semiconductor nanostructure with large metallic electrodes deposited on top of the nanostructure.[4−11] Hitherto, theoretical interpretation of such experiments has often been based on transport and electronic structure calculations for isolated nanostructures, ignoring the influence of the electrodes. When the electrode is included in the calculation, its effects are often described by a short-range correlation theory such as local density approximation (LDA).[12] However, the electrode introduces a long-range correlation effect (which in the static limit is the interactions with metal surface image charges) well into the semiconductor nanowire. These long-range correlations are absent from LDA and can only be addressed by many-body theories such as the GW (in this acronym, G stands for the Green's function and W is the screened Coulomb interaction). Recently the influence of the metallic surface on the electronic states of an absorbed benzene molecule has been studied with the GW model,[13] where significant reduction of the band gap was found. Similar effects were also studied using a simple model[14] for a single-molecule transistor, where the possibility of a localized state due to the image potential is demonstrated.

In this letter, we study the long-range correlation effects in the CdSe nanorod in contact with a metallic electrode. Nanorod contact exemplifies a different regime than that of the small organic molecules studied before. Unlike in the molecules, the phenomenon described here does not depend on the details of a contact structure on the atomic level (which often cannot be controlled experimentally). In addition, the dielectric screening of the rod itself plays an important role in determining the image charge and one can also show how the contact evolves from the nanorod to a bulk interface. We show that the surface polarization potential is surprisingly large, particularly for small nanostructures, where it alters the familiar electronic structure and gives rise to a nanocontact phenomenon: electrode-induced wave function localization. We show the trend of the localization, decreasing with nanostructure size and vanishing when the system becomes large, which explains why it has been overlooked in the past. We assume that the metal electrode makes a Schottky contact with semiconductor nanorod.[15] In the quasi-1D geometry, the depletion region width depends exponentially on doping[16] and is much longer than the nanorod size for nondegenerate doping or undoped nanorod. Therefore, there is very limited charge transfer between the electrode and the rod, which therefore is ignored here. We will start with the GW equation and derive a simplified Schrödinger equation under a static approximation. This simplified equation will then be solved using atomistic pseudopotential method.

A single-particle wave function can be obtained from the GW quasiparticle equation[17]

$$H_0\psi_i(r) + \int \mathrm{d}^3r'\Sigma(r,r';E_i)\psi_i(r) = E_i\psi_i(r) \qquad (1)$$

where H_0 is a Hartree Hamiltonian, and the nonlocal potential Σ (self-energy) within GW is approximated as

* Corresponding author. E-mail: dodemchenko@lbl.gov.

10.1021/nl072027n CCC: $37.00
Published on Web 09/21/2007

$$\Sigma(r,r';\omega) = -\sum_{i}^{occ} \psi_i(r)\psi_i^*(r') f_i W(r,r';\omega - \epsilon_i) + \frac{1}{\pi}\sum_{i}^{occ} \psi_i(r)\psi_i^*(r') \int_0^\infty d\omega' \frac{\mathrm{Im}W(r,r';\omega')}{\omega - \epsilon_i - \omega' + i\delta} \quad (2)$$

where the first and second terms are the screened-exchange Σ^{SX} and the Coulomb-hole Σ^{CH} terms, respectively, f_i is the Fermi−Dirac occupation for the state ψ_i, and W is the screened Coulomb potential $W(r,r';\omega) = d^3r''\epsilon^{-1}(r,r'',\omega)/|r'' - r'|$ (ϵ^{-1} is the inverse dielectric function). In a nanocrystal, it can be shown that the self-energy can be divided into the bulk and surface contributions $\Sigma = \Sigma_{bulk} + \Sigma_P$, following the screened Coulomb potential separation $W(r,r';\omega) = W_{bulk}(r,r';\omega) + P(r,r';\omega)$. As a result, the GW equation (eq 1) becomes

$$H_{bulk}^{GW}\psi_i(r) + \int d^3r'\Sigma_P(r,r',\epsilon_i)\psi_i(r') = \epsilon_i\psi_i(r) \quad (3)$$

Here, H_{bulk}^{GW} is a bulk-like GW Hamiltonian in the nanostructure and a free electron Hamiltonian in the surrounding vacuum. Under a static approximation (dropping the ω dependence in $\Sigma_P(r,r';\omega)$) taking into account $\Sigma_P = \Sigma_P^{SX} + \Sigma_P^{CH}$, one can prove[18] that

$$\int d^3r'\Sigma_P^{SX}(r,r')\psi_j(r') = -2f_iP(r)\psi_j(r') \quad (4)$$

$$\int d^3r'\Sigma_P^{CH}(r,r')\psi_j(r') = P(r)\psi_j(r') \quad (5)$$

where $P(r)$ is the surface polarization potential

$$P(r) = \frac{1}{2}\lim_{r'\to r}[W_{nano}(r',r) - W_{bulk}(r',r)] \quad (6)$$

Here $W_{nano}(r',r)$ is the screened electrostatic potential in the system (including electrode) at r' created by a test charge at r, and $W_{bulk}(r',r)$ is a corresponding potential in the bulk. Therefore, the quasiparticle equation is reduced to

$$H_{bulk}^{GW}\psi_i(r) + (1 - 2f_i)P(r)\psi_i(r) = \epsilon_i\psi_i(r) \quad (7)$$

For a few thousand atom nanostructure, the H_{bulk}^{GW} (which has a bulk-like short-range Σ_{bulk}) can be represented by an atomistic empirical pseudopotential, which is accurately fitted into the experimental bulk band structure. Therefore, finally we obtain the following equation derived from the static approximation of GW equation

$$\left\{-\frac{1}{2}\nabla^2 + V + (1 - 2f_i)P(r)\right\}\psi_i(r) = \epsilon_i\psi_i(r) \quad (8)$$

where the potential V is the semiempirical pseudopotential (SEPM).[19] The eq 8 can be solved by using the folded spectrum method (FSM) for a few states near the band gap.[20] The use of static approximation in the GW method has been shown to be adequate for a benzene molecule on the metal surface.[13] It has also been shown that this approximation is adequate in a bulk metal/semiconductor contact.[21] Thus, there is a good reason to believe it is also sufficient in a nanocontact, an intermediate case.

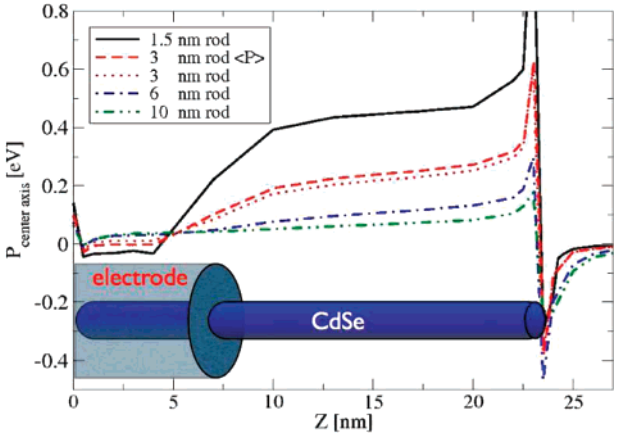

Figure 1. Polarization potential $P(z)$ as a function of the z-coordinate along the nanorod center axis. The nanorod is embedded into the electrode by a quarter of its length, nanorods of diameter 1.5, 3, 6, and 10 nm are used. Inset: Example of the modeled electrode and CdSe nanorod used in the present work. (Electrode diameter is not to scale.)

To find the electrostatic potential $W(r',r) \equiv \phi_{r'}(r)$, we solve the Poisson equation for the structure shown in Figure 1

$$\nabla[\epsilon(r)\nabla\phi_{r'}(r)] = 4\pi\rho_{r'}(r) \quad (9)$$

Here $\rho_{r'}(r)$ is a unit test charge density of a narrow (0.15 nm) Gaussian distribution centered at r', and final result $P(r)$ does not depend on it. The dielectric function $\epsilon(r)$ is modeled by following our study of dielectric response of a nanostructure,[22] which equals $\epsilon_{CdSe} = 10$ at the center of the nanorod and approaches 1 near the surface of the rod.

The procedure for the calculations is the following: (i) compute potential $V(r)$ from the semiempirical atomic pseudopotentials for an isolated nanorod (including passivating atoms); (ii) compute $P(r)$ on a 3D mesh by solving eq 9 for the same geometry of the nanorod, now including a metallic electrode as a continuous medium with an exceedingly large dielectric constant (no atomistic calculation of the electrode is necessary); (iii) add $V(r)$ and $P(r)$ for the nanorod and perform one shot non-self-consistent FSM calculation (solve eq 8) for the eigenvalues and the wave functions around the band gap.

We calculated surface polarization potential $P(r)$ for a nanorod length of 23 nm, and the diameters of 1.5, 3, 6, and 10 nm. The diameter of the electrode was much larger than that of the nanorod ($d_{electr} = 23$ nm) in order to mimic a typical experimental setup. The SEPM calculations were performed for CdSe nanorods in the wurtzite crystal structure, length of 23 nm, and 3 nm diameter, with a total number of atoms of 5434 for a series of contact depths.

Figure 1 shows the polarization function $P(z)$ as a function of the z-coordinate running along the nanorod central axis for nanorod diameters ranging from 1.5 to 10 nm, in the

case of the nanorod embedded into the electrode by a quarter of its length. For the 3 nm rod, we also computed the weighted average $\langle P(z)\rangle = \int |\psi_i(x,y)|^2 P(r)\, dx dy$, where $|\psi_i(x,y)|^2 = \int |\psi_i(r)|^2\, dz$ is either as a conduction band minimum (CBM) or valence band maximum (VBM) wave function. The $\langle P(z)\rangle$ is a measure of the effective influence of the $P(r)$ on the relevant wave functions, and for the 3 nm rod, the central axis $P(z)$ and the weighted average $\langle P(z)\rangle$ are practically the same.

The $P(r)$ has contributions from both the electrode and nanorod itself. While the electrode produces a large confining potential in the embedded region, the nanorod produces a nearly constant nonzero $P(r)$ value arbitrarily far away from the electrode due to interaction with image charges on the surface of the nanorod itself. Thus, even in the absence of the electrode, $P(r)$ of the free nanorod has a finite value, which increases as nanorod diameter decreases and influences its energy spectrum and charging properties.[18] The $P(r)$ peaks across the interfaces where the dielectric function $\epsilon(r)$ in eq 9 changes rapidly, as for example in the vicinity of $z \rightarrow z_{rod}$ in Figure 1. Outside of the nanorod, the $P(r)$ quickly approaches zero. The electrode influence decreases with increased nanorod diameter. At 10 nm diameter, a drop of $P(r)$ near the electrode is almost indiscernible. This indicates that the localization effect that will be discussed below does not exist in a macroscopic contact, which is why this has been overlooked in large nanostructures (but observed in single molecules[14]). Our study indicates that when the diameter d is smaller than 3 nm, the localization potential becomes appreciable. Note that single-molecule systems, as those in refs 13 and 14, cannot be used to study this size dependence. This size dependence is also related to the fact that our rod is partially embedded in the electrode, a common experimental setup, which is not the case for the molecules absorbed on the metal surface. For small nanorods, the effect is surprisingly large, the $P(r)$ provides a strong confining potential for electrons or holes (about 0.5 eV for 1.5 nm nanorod), and leads to an electrode-induced electron/hole localization. The enhancement of the effect on the nanoscale is important. In a bulk metal/semiconductor contact, there is also a "band gap reduction" potential.[21] However, that effect, which corresponds to a kink near the contact in Figure 1, is very weak and exists for all nanorod sizes in our case.

Figure 2 shows the real space contour plots of the three wave functions adjacent to the band gap in the 3 nm CdSe quantum rod conduction and valence band. In Figure 2a, three wave functions are calculated for a free-standing CdSe nanorod, while for Figure 2b, the nanorod is embedded into the electrode by one-quarter of its length. In the latter case, both CBM and VBM wave functions are localized by the surface polarization potential induced by the electrode. While for CBM states, the wave functions are just shrunk in the z-direction, the second and third VBM states show different nodal structure in comparison with their free-rod counterparts, indicating strong state mixing and crossing. Because of this localization, the transport properties of small nanorods measured with attached electrodes will be different from a

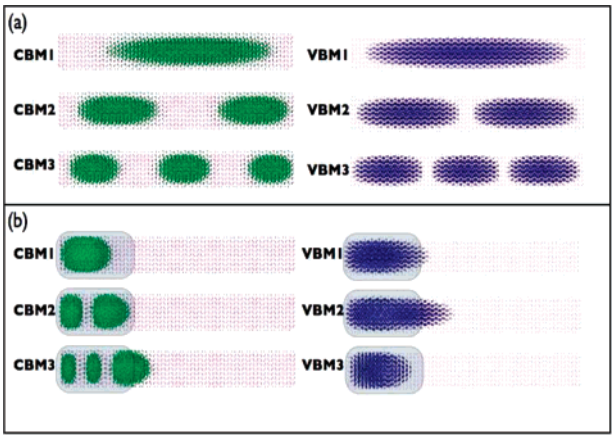

Figure 2. Contour plots of the CBM and VBM wave functions for the 3 nm diameter CdSe nanorod, for (a) the free-standing nanorod, (b) the nanorod with an electrode covering one-quarter of its length. The semitransparent rectangles indicate the position of the electrode.

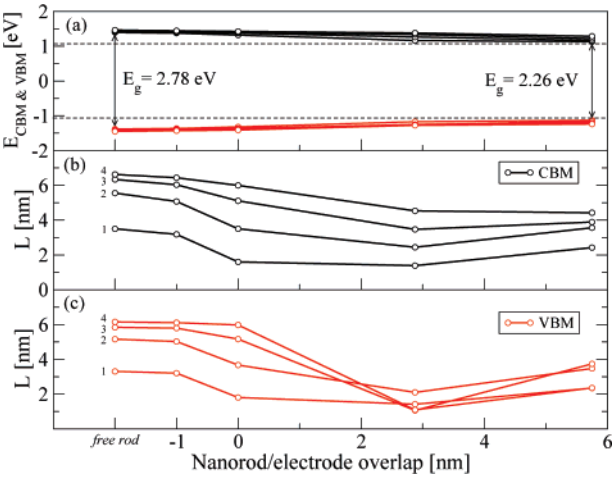

Figure 3. Evolution of the electronic states for the 3 nm diameter CdSe nanorod as a function of the nanorod/electrode overlap: (a) CBM and VBM eigenvalues (band gap), dashed lines indicate the band gap computed ignoring surface polarization potential; (b) and (c) localization function (defined in the text) for the CBM and VBM states, respectively.

familiar free electron-like picture and may resemble the case of the Coulomb blockade.

Another important consequence of the electrode surface polarization potential is the change in the value of the band gap. Figure 3 shows the VBM and CBM states evolution as a function of the overlap between the nanorod and the electrode for the 3 nm diameter CdSe nanorod. In this case, the value of the band gap is reduced by approximately 0.5 eV (Figure 3a), from 2.78 to 2.26 eV, as the rod is embedded into the electrode. In the absence of the electrode, the polarization potential $P(r)$ of a free-standing nanorod induces the band gap increase of 0.54 eV (from 2.24 to 2.78 eV) in comparison with the gap calculated by ignoring the surface polarization (dashed lines in Figure 3).

To quantify the electrode-induced localization of the electron and hole wave functions, we define a localization function $L^2 = \int |\psi_i(r)|^2 (z - z_0)^2\, dr$, where the wave function center of mass is $z_0 = \int |\psi_i(r)|^2 z\, dr$. It shows how spread

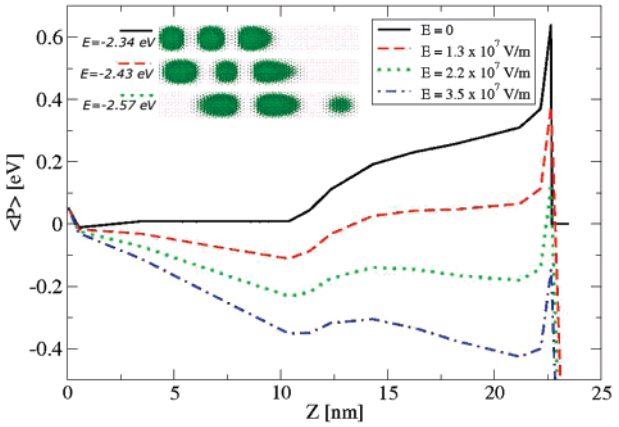

Figure 4. Weighted average of the polarization function $\langle P(z)\rangle$ for 3 nm diameter CdSe nanorod, half-covered by the electrode, for several values of applied external electric field. The inset shows the real space contour of the CBM3 wave function along with their eigenvalues for the electric fields of 0, 1.3, and 2.2 $\times$ 10^7 V/m.

out the wave function is throughout the nanorod. This localization is presented in parts b and c of Figure 3 for CBM and VBM, respectively, as a function of the electrode/nanorod overlap. The localization of the wave functions is different from that of the free-standing nanorod already when the nanorod and the electrode are 1 nm apart and becomes significant when the electrode is in contact with the nanorod. Throughout the electrode/nanorod overlap range, the electron states are less localized than the hole states due to the differences in their effective masses.

To make carriers mobile again, one can apply an electric field along the wire axis to overcome the wave function localization. To estimate the magnitude of this electric field, we apply a linear potential drop to the total potential $V(r)$ in eq 8 between the ends of the nanorod and calculate the resulting electronic properties. This is demonstrated in Figure 4, where the weighted average of the polarization potential $\langle P(z)\rangle$ is plotted for a 3 nm diameter CdSe nanorod embedded into the electrode by half of its length. The field of 2.2 $\times$ 10^7 V/m (bias voltage of about 0.5 V applied across the 23 nm nanorod) is needed to delocalize the CBM wave function. The inset shows a representative (the third) CBM wave function contour plots for electric fields of 0, 1.3, and 2.2 $\times$ 10^7 V/m (bias voltages of 0, 0.3, and 0.5 V). The wave function in the latter case is dragged by the field toward the center of the rod, while its eigenvalue changes from -2.34 to -2.57 eV.

In conclusion, by using a GW derived atomistic pseudopotential equation, we have demonstrated the electrode-induced localization of CBM and VBM states in CdSe nanorods. The effect is surprisingly large for small (1.5−3 nm diameter) nanorods but becomes insignificant as nanorod size grows (6 nm and up). The large polarization potential $P(r)$ induced by the electrode also lead to the narrowing of the quasiparticle band gap by 0.5 eV in 3 nm CdSe nanorods. The wave function localization effect might change the electron transport picture in the nanorod (wire), e.g., from a free carrier picture to Coulomb blockade picture. This is a unique nanocontact phenomenon absent in its macroscopic counterpart.

To experimentally confirm the effect of electrode-induced localization, we propose a measurement using one of the established wave function mapping techniques, such as scanning tunneling microscopy (STM), along with conductivity measurements for a series of small nanorods (1.5−3 nm diameter) with varying contact depths.

Acknowledgment. This work was supported by U.S. Department of Energy, BES, Office of Science, under contract no. DE-AC02-05CH11231 and used the resources of the National Energy Research Scientific Computing Center (NERSC).

References

(1) Manna, L.; Milliron, D. J.; Miesel, A.; Scher, E. C.; Alivisatos, A. P. *Nat. Mater.* **2003**, *2*, 382.
(2) Milliron, D. J.; Hughes, S. M.; Cui, Y.; Manna, L.; Li, J.; Wang, L. W.; Alivisatos, A. P. *Nature* **2004**, *430*, 190.
(3) Gao, P.; Wang, Z. L. *J. Phys. Chem. B* **2002**, *106*, 12653.
(4) Klein, D. L.; Roth, R.; Lim, A. K. L.; Alivisatos, A. P.; McEuen, P. L. *Nature* **1997**, *389*, 699.
(5) Fang, L.; Park, J.; Cui, Y.; Schrier, J.; Lee, B.; Wang, L.-W.; Alivisatos, A. P.; Salmeron, M. *J. Chem. Phys.* **2007**, in press.
(6) Steiner, D.; Mokari, T.; Banin, U.; Millo, O. *Phys. Rev. Lett* **2005**, *95*, 055805.
(7) Heo, Y. W.; Tien, L. C.; Norton, D. P.; Kang, B. S.; Ren, F.; Gila, B. P.; Pearton, S. J. *Appl. Phys. Lett.* **2004**, *85*, 2002.
(8) Cui, Y.; Banin, U.; Björk, M. T.; Alivisatos, A. P. *Nano Lett.* **2005**, *5*, 1519.
(9) Thelander, C. *Appl. Phys. Lett.* **2003**, *83*, 2052.
(10) Zhang, Y.; Ichihashi, T.; Landree, E.; Nihey, F.; Lijima, S. *Science* **1999**, *285*, 1719.
(11) Gudiksen, M. S.; Lauhon, L. J.; Wang, J.; Smith, D. C.; Lieber, C. M. *Nature* **2002**, *415*, 617.
(12) Landman, U.; Barnett, R. N.; Scherbakov, A. G.; Avouris, P. *Phys. Rev. Lett.* **2004**, *85*, 1958.
(13) Neaton, J. B.; Hybertsen, M. S.; Louie, S. G. *Phys. Rev. Lett.* **2006**, *97*, 216405.
(14) Kubatkin, S.; Danilov, A.; Hjort, M.; Cornil, J. J.-L. B.; Stuhr-Hansen, N.; Hedegård, P.; Bjørnholm, T. *Nature* **2003**, *425*, 698.
(15) Léonard, F.; Talin, A. A. *Phys. Rev. Lett.* **2006**, *97*, 026804.
(16) Léonard, F.; Tersoff, J. *Phys. Rev. Lett.* **1999**, *83*, 5174.
(17) Hedin, L.; Lundquist, S. In *Solid State Physics*; Academic Press: New York, 1969; p 1.
(18) Wang, L. W. *J. Phys. Chem. B* **2005**, *109*, 23330.
(19) Wang, L. W.; Zunger, A. *Phys. Rev. B* **1996**, *53*, 9579.
(20) Wang, L. W.; Zunger, A. *J. Chem. Phys.* **1994**, *100*, 2394.
(21) Inkson, J. C. *J. Phys. C* **1973**, *6*, 1350.
(22) Cartoixa, X.; Wang, L. W. *Phys. Rev. Lett.* **2005**, *94*, 236804.

NL072027N